AUTOMATIC CRACK DETECTION ON ROAD IMAGERY USING ANISOTROPIC DIFFUSION AND REGION LINKAGE

Henrique Oliveira[1,2] and Paulo Lobato Correia[1]

[1]Instituto de Telecomunicações – Instituto Superior Técnico
[2]Escola Superior de Tecnologia e Gestão – Instituto Politécnico de Beja
Torre Norte - piso 10, Av. Rovisco Pais, 1, 1049-001, Lisboa, Portugal
phone: + (351) 218418454, fax: + (351) 218418472, email: {hjmo, plc}@lx.it.pt

ABSTRACT

A novel strategy to automatically detect cracks in road pavement surface imagery, acquired by a laser imaging system, is proposed. It includes a new procedure to link fragments of crack regions based on a maximum a posteriori (map) classifier, which relies on a set of geometric characteristics of the segmented binary regions.
The proposed system starts with an anisotropic diffusion filtering, to smooth image texture variations resulting from the type of sensor used. Then, a Gaussian function is used to model the histogram for pixels intensities below a certain value, which allows inferring the threshold level to be used for image segmentation. Next, less relevant binary regions are identified, being kept only if they are linked to relevant crack regions.
Encouraging experimental crack detection results are presented based on real images captured along Canadian roads.

1. INTRODUCTION

Crack detection in images is an active research topic, as cracks are the most common road surface distress type being evaluated by inspectors during road surveys. Recent approaches to automatic crack detection systems includes the usage of neural networks [1] or Markov random fields [2], among others [3].
This paper proposes a new crack detection approach based on: image smoothing; automatic segmentation by thresholding; a new procedure to link the resulting binary regions and to decide whether or not to label them as cracks.
The nature of pavement surface images acquired by automated survey systems like INO's 4K model using its laser road imaging system (LRIS) [4], poses some challenges to the automatic detection of crack distresses, due to the texture characteristics they present [5]. Cracks usually correspond to image regions with the following characteristics: very dark intensities when compared to the surroundings; linear shape development, with variable width.
Texture smoothing of pavement surface images can be very useful in automatic crack detection systems, allowing subsequent segmentation by thresholding to better distinguish crack regions from the textured image background. Anisotropic diffusion is a well known filtering technique, mainly used for smoothing and restoration purposes [6], introduced by Perona and Malik in image processing for scale-space description and edge detection [7], as it smoothes image regions, while preserving and enhancing the contrast at sharp intensity gradients [8]. Its application for image smoothing is well known in [9] [10]. Anisotropic diffusion has also recently been applied, with a generalized diffusion coefficient function, for defect detection in low-contrast surface images [11].
Thresholding is one of the simplest and computationally fast region-based segmentation processes, being especially useful when dealing with large images, as those considered in the present application, and used to generate the experimental results presented in section 3. Its usage allows to significantly reduce the computational effort required for the crack detection task.
In this paper thresholding is used as a simple classification procedure, with pixels being labelled '0' (non-crack) if their intensities are above a certain gray level, and '1' (crack) otherwise. Candidate crack regions are then identified using a connected components algorithm. Since several connected components may belong to the same crack, as cracks usually present a linear shape development, a *map* classifier is proposed to identify groups of crack regions that effectively belong to the same crack, relying on a three-dimensional feature space exploiting a set of geometric characteristics of those connected components.
The paper is organized as follows: in section 2, the proposed automatic crack detection strategy is described. Section 3 gives experimental results and analyses the behaviour of the system on a real image database, taken by INO's 4K model during a real road flexible pavement survey over a Canadian road. Section 4 summarizes the contributions of the paper and presents some hints for future work.

2. SYSTEM ARCHITECTURE

The system architecture of the proposed automatic crack detection strategy, using flexible road pavement surface images, is presented in Figure 1. The details of the main processing blocks are provided in the following.

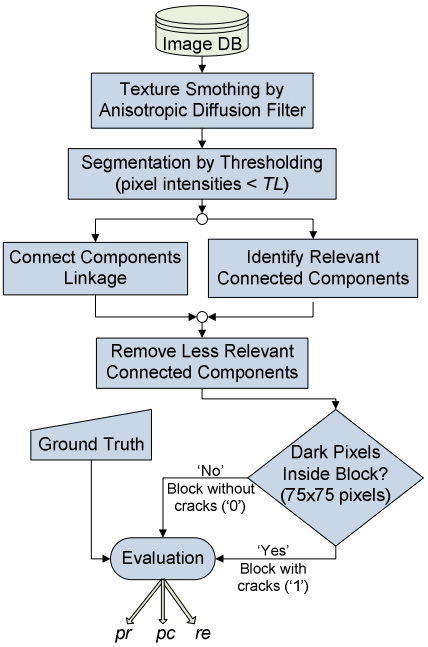

Figure 1: System architecture.

2.1 Texture smoothing by anisotropic diffusion filtering

INO's LRIS 4K model is composed of two sets of linescan sensors and lasers covering a road section of up to 4 m wide. Each linescan sensors captures images of size 4096×2048 pixels (length×width), with a spatial resolution of 1 mm^2, and gray-level intensities ranging from 0 to 255. Sample acquired images are shown in Figure 2.

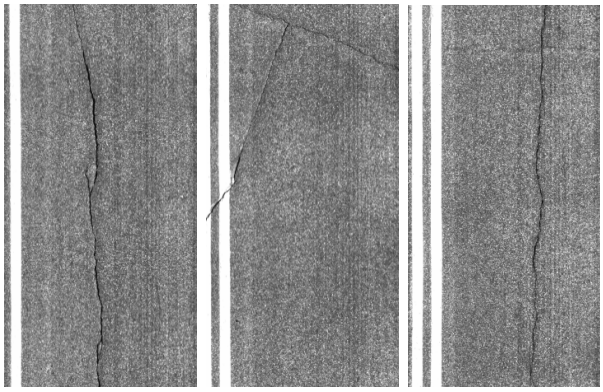

Figure 2: Samples road surface images acquired by LRIS.

Pavement surface images acquired by INO's LRIS 4K model present a remarkably random texture, with a considerable variance of pixels intensities, as can be verified analysing of the left plot of Figure 3. This texture randomness makes the automatic detection of cracks a difficult task, as several and sparse dark areas would result if using a simple and fast segmentation method, like thresholding, to distinguish between the image background and crack regions.

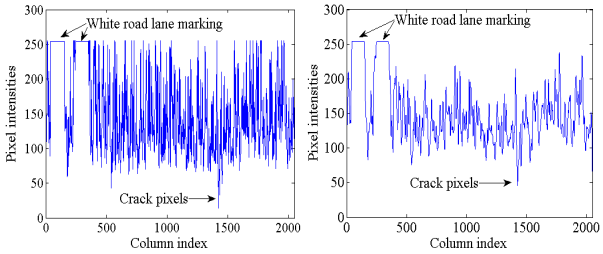

Figure 3: Line 500 of the right image shown in Figure 2: original pixels values (left) and after anisotropic diffusion filtering (right).

In this paper smoothing is tested using two anisotropic diffusion models [7] [8]: the first model favours high contrast edges over low contrast ones; the second favours wide regions over smaller ones. Evaluation results using both methods are presented in section 3, varying the number of iterations from 1 to 12, and the conduction coefficients from 20 to 100, with step 10. The right plot of Figure 3 shows the anisotropic diffusion filtering result, for the right image in Figure 2, using 12 iterations and a conduction coefficient of 60. This result shows a considerable pixels intensity variance reduction, achieved by the proposed filtering technique, without significantly deteriorating the crack information, as it corresponds to the darker areas of the LRIS images.

2.2 Segmentation by thresholding

Thresholding is one of the simplest and computationally faster segmentation procedures, being selected to identify crack regions present in the pavement surface images taken during road surveys.

For each original image, an intensity value (i_{img}) is calculated using the Otsu algorithm [12] and a histogram is computed using only the intensities lower than i_{img}. The corresponding histogram for the right image of Figure 2 is presented in Figure 4. Then, a Gaussian function is fit to the histogram bins located to the left side of its maximum value. The analysis of Figure 4 shows a well fitted Gaussian function (red line), with the black point representing the Gaussian mean value estimate (96.9). Then, a threshold value is computed (*TL*), so that $P(TL) \approx 95.5\%$, which corresponds to $TL = \mu - 2\times\sigma$. A practical example is given by the blue line drawn in Figure 4, with $P(57.7) \approx 95.5\%$.

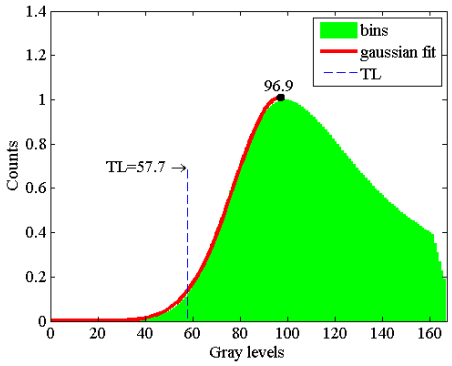

Figure 4: Histogram of the right image of Figure 2 and the fitted Gaussian function.

TL is the threshold value used to segment the filtered image. Pixels with intensity lower than *TL* are labelled '1' (crack pixels), the remaining receiving label '0' (non-crack pixels). Figure 5 presents sample results for a zoomed area (with dimensions of 400×500 pixels) of the right image of Figure 2.

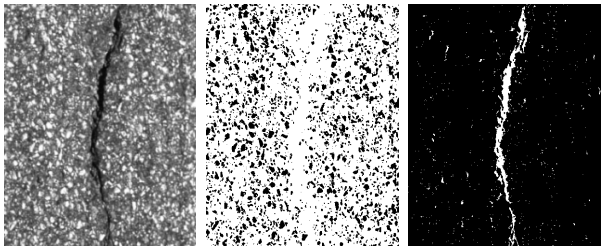

Figure 5: Original image (left); selection of pixels with intensities lower than i_{img} (middle); crack pixels using the proposed method, after thresholding the filtered image using *TL* (right).

It can also be noted that, in the images acquired by INO's 4K model, white road lane marks correspond to regions with high and quite consistent gray level intensities (typically ranging from 252 to 255). The proposed thresholding procedure is robust to their presence, excluding them from the computed histogram (see Figure 4), not requiring any special handling procedure, as sometimes found in the literature – for instance a thresholding followed by the application of a Hough transform is required in [1].

2.3 Identify relevant connected components

Candidate crack pixels are then grouped using a connected components algorithm, to form a set of connected component objects (*cco*). The right image of Figure 5 reveals the presence of very small and sparse *cco*s, many of them not corresponding to real road cracks. In fact, only *cco*s respecting a set of conditions should be selected by the system as crack regions.

To be kept as a candidate crack region a *cco* should have: (i) more than 90% of eccentricity for an ellipse fitted to it; (ii) width higher than or equal to 2 mm (computed dividing the number of pixels in the *cco* by the number of pixels in its skeleton); (iii) major axis of a fitted ellipse longer than 25 pixels. Figure 6 presents sample results after removal of the less relevant connected components, for the right image of Figure 5.

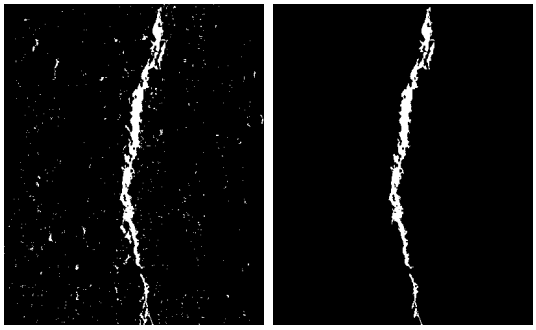

Figure 6: Removal of the less relevant connected components: original image (left); processed image (right).

2.4 Connected components linkage

The less relevant *ccos* considered for removal in the previous operation, might be spatially connected to other relevant crack regions. In that case, they should also be considered as crack components, as this type of pavement surface distress typically develops along a given direction, thus presenting a linear shape.

The solution adopted to keep these less relevant *ccos* (binary regions), linking them to others belonging to the same crack, is based on a *map* classifier.

Let $i, j \in \{1, \ldots, m\}$ be the *cco*'s indexes, with m being the number of available connected components in a given binary image. The total number of connected component pairs will be $m!/(2\times(m\text{-}2)!)$, and each pair can be identified by cc_{ij}, with $i \neq j$.

The proposed linkage procedure comprehends the comparison between all the available pairs of connected components, evaluating their spatial proximity and linear shape development. The considered pattern recognition system uses three simple but effective features: $x1_{ij}$, the shortest distance between the connected components; $x2_{ij}$, the smallest angle between fitted ellipses major axis orientations; $x3_{ij}$, the smallest angle between the orientation of the line segment connecting the two *cco*'s centroid and the orientation of the major axis of an ellipse that has the same normalized second central moments as region i. Each cc_{ij} will be classified as belonging either to classe c_1, a 'linked' cc_{ij}, or to class c_2, a 'not linked' cc_{ij}.

Thus, each cc_{ij} is' linked' when the following condition holds true:

$$P\left(c_1 \mid \vec{X}\right) > P\left(c_2 \mid \vec{X}\right), \text{ with } \vec{X} = \begin{bmatrix} x1_{ij} \\ x2_{ij} \\ x3_{ij} \end{bmatrix}. \qquad (1)$$

Taking into account the Bayes theorem, condition (1) is rewritten,

$$p\left(\vec{X} \mid c_1\right) \times P\left(c_1\right) > p\left(\vec{X} \mid c_2\right) \times P\left(c_2\right), \qquad (2)$$

where p stands for the probability density function and $P(c_1)$ and $P(c_2)$ are respectively the *a priori* probabilities of classes c_1 and c_2. Assuming a Gaussian distribution for each random variable $x1_{ij}$, $x2_{ij}$ and $x3_{ij}$, i.e. $N_1(\mu 1,\sigma 1)$, $N_2(\mu 2,\sigma 2)$ and $N_3(\mu 3,\sigma 3)$ respectively, and also the conditional independence of those random variables, the respective three-dimensional mean vectors and covariance matrices are,

$$\vec{\mu}_k = \begin{bmatrix} \mu 1_k \\ \mu 2_k \\ \mu 3_k \end{bmatrix} \quad \text{and} \quad \text{cov}\left\{\vec{X}\right\}_k = \begin{bmatrix} \sigma 1_k & 0 & 0 \\ 0 & \sigma 2_k & 0 \\ 0 & 0 & \sigma 3_k \end{bmatrix}, \qquad (3)$$

where k is the class index, with $k \in \{1,2\}$. Finally, condition (2) is rewritten using the definitions in (3), leading to expression (4). Thus, two regions are considered 'linked' (a cc_{ij} classified into class c_1) when condition (4) holds true:

$$\sum_{n=1}^{3}\left(\log \sigma n_1 + \left(\frac{xn_{ij} - \mu n_1}{\sigma n_1}\right)^2\right) - \log\left(P(c_1)\right) < \sum_{n=1}^{3}\left(\log \sigma n_2 + \left(\frac{xn_{ij} - \mu n_2}{\sigma n_2}\right)^2\right) - \log\left(P(c_2)\right), \qquad (4)$$

where n is the number of features used. Linked binary regions can then be merged with relevant crack regions, obtained using the procedure described in section 2.3. Some of the less relevant regions can thus be kept as 'crack regions', if linked to other relevant crack regions, rather than being removed.

For tuning the binary region linkage procedure, a supervised strategy was adopted. Instead of computing both terms in (4), only the left one is calculated from the set of regions under analysis, as illustrated in Figure 7 (top-left), where a portion of a randomly chosen image is represented. The value for the second term in (4) was empirically chosen, after exhaustive testing, to allow achieving the results considered as ground truth. Equal *a priori* probabilities for classes c_1 and c_2 were considered during the tuning procedure.

The candidate crack regions, after segmentation using *TL*, are shown in the top-left image. The output of the proposed connected components linkage procedure is presented in the top-right image, with each colour identifying a different linear object, composed by several linked regions, with a total of five different linear objects found. The relevant crack regions, selected using the procedure outlined in section 2.3, are shown in the bottom-left image.

The bottom-right image shows the final crack regions identified, merging the connected components using relevance and linkage information. In this example, two additional crack regions were selected (the two small regions labelled '1' and '2') as they are linked to other relevant crack regions.

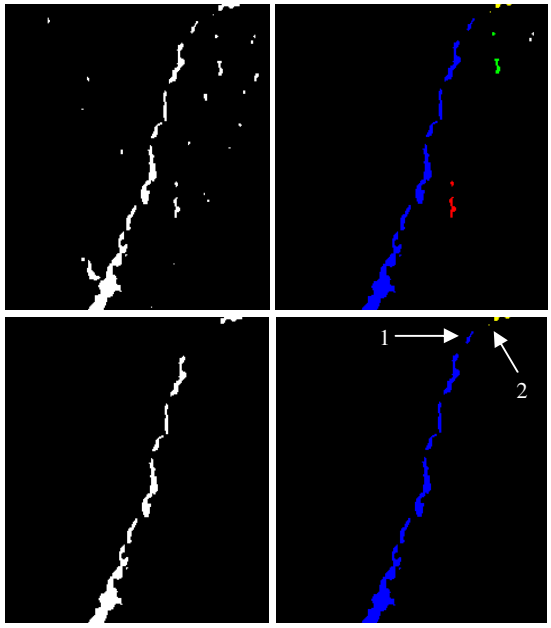

Figure 7: Connected components linkage results.

3. EXPERIMENTAL RESULTS

The proposed automatic crack detection methodology has been tested on images captured during a real road pavement survey in Canada. Experimental results are presented using 20 images for which a ground truth is available, provided by a skilled inspector

who has manually identified the existing crack regions.

The two laser illuminators of INO's LRIS 4K model provide images with a constant illumination, originating stable Gaussian mean values estimates, ranging between 92 and 101. Additionally, the automatically computed threshold values, *TL*, are also quite stable, taking values in the range from 54 to 62 (see Figure 8).

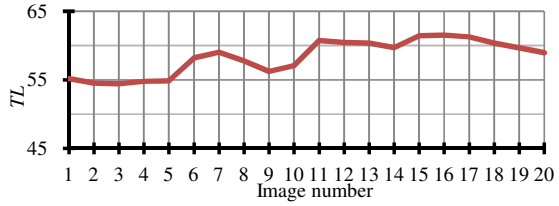

Figure 8: Plot of *TL* values for the 20 images for which ground truth results are available.

216 simulations were run using the two anisotropic diffusion filter models mentioned in section 2.1 (108 simulations for each model), with the conduction coefficients (*CondCoef*) ranging from 20 to 100 with step 10, and considering between 1 and 12 iterations for each conduction coefficient value. Each simulation is evaluated using a set of well known metrics, to evaluate the crack detection system performance: recall (*re*), the ratio between the number of blocks correctly classified as cracks and the total number of ground truth crack blocks; precision (*pr*), the ratio between the number of blocks correctly classified as cracks and the total number of crack blocks detected; performance criterion (*pc*):

$$pc = (2 \times re \times pr) \div (re + pr). \quad (5)$$

In a road surface crack detection application, *re* is the most important metric, as missing existing cracks is often more critical than presenting a few false positives. Thus, a modified *pc* metric can be considered to emphasize the relevance of *re*, according to:

$$pc_{mod} = (2 \times re \times pr) \div (re \times cf_1 + pr \times cf_2), \quad (6)$$

where cf_1 and cf_2 are cost factors.

Figure 9 shows simulations results in terms of pc_{mod} values (with parameters $cf_1=0.5$ and $cf_2=1.5$, empirically chosen by the system operator), for the second anisotropic diffusion model, the one presenting more stable *re* and *pr* values and consequently also less variant pc_{mod} values, foreseeing its preference when compared to the first model. For *CondCoef* values ranging between 60 and 100, the curves representing pc_{mod} are almost superimposed, showing only small variations (see Figure 9-top). Moreover, adopting higher *CondCoef* values, the maximum value in each pc_{mod} curve shifts slightly to the left, foreseeing less iterations of the anisotropic diffusion algorithm, thus favouring the computational load of the approach proposed in this paper (see Figure 9-bottom).

Figure 10 presents a comparison, between the original *pc* metric (5) and the alternative formulation presented in (6), again with parameters $cf_1=0.5$ and $cf_2=1.5$ As can be observed, the second metric (pc_{mod}) is more biased towards *re*, which can be more interesting for crack detection applications. In this case, the best *pc* value corresponding to a conduction coefficient ranging between 60 and 100 is 93.8%, obtained when *CondCoef* is equal to 60, with *re* and *pr* being respectively 96.3% and 86.9%, with 4 iterations. Adopting a *CondCoef* equal to 100, best pc_{mod} value is now 93.5%, with *re* and *pr* being respectively 97.2% and 84.0%, with 3 iterations. Execution times for a complete image of 4096×2048 pixels, using a Intel Core i5-750 processor running the Windows 7 operating system (*OS*), were less than three minutes, with 4 iterations of the anisotropic diffusion algorithm.

Concerning the proposed connected components linkage procedure, the *maximum à posteriori* classifier performs quite well. This is illustrated in Figure 11, which includes results for several zoomed areas of the middle image of Figure 2. Less relevant binary crack regions which would be discarded by the procedure described in section 2.3, are re-evaluated and those presenting a greater probability of being connected to a relevant crack are kept as part of the final set of crack regions detected.

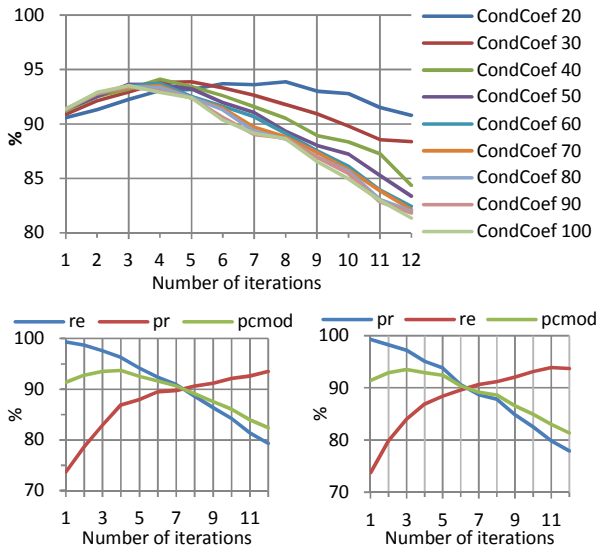

Figure 9: pc_{mod} values for conduction coefficients ranging from 20 to 100, for each iteration, using the second anisotropic diffusion model (top), and *re*, *pr* and pc_{mod} values computed for conduction coefficients of 60 (bottom-left) and 100 (bottom-right).

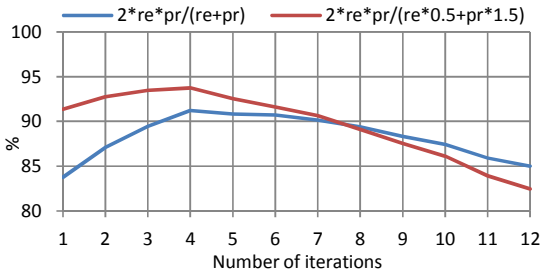

Figure 10: Comparison between *pc* and pc_{mod} values, for cost factors cf_1 and cf_2,of {0.5, 1.5}, using the second anisotropic diffusion model and a *CondCoef* of 60.

4. CONCLUSIONS AND FUTURE WORK

This paper proposes a new automatic system to detect cracks in images captured during real pavement surveys. The system performs well and it is robust to the presence of white road lane markings, not requiring any special procedure to find those areas, as sometimes found in the literature [1]. Very good results are obtained for *re*, *pr* and pc_{mod}, notably when taking into account the difficulty of the task, even for a human observer. In fact, the variation of estimates among different human operators typically leads to a result uncertainty between 1% to 2%, mostly due to the experienced human ambiguity in recognizing patterns [13].

As future work, the use of other methods to reduce the high variance of pixels intensities without significantly deteriorating the information about cracks, like the UINTA filtering strategy [14], will be considered. Moreover, the inclusion of radiometric properties in the binary regions linkage process instead of only a set of the geometric ones, to infer about the existence of pixels between detected crack regions that could be retrieved to better connect them, and a better training procedure, will be taken into account.

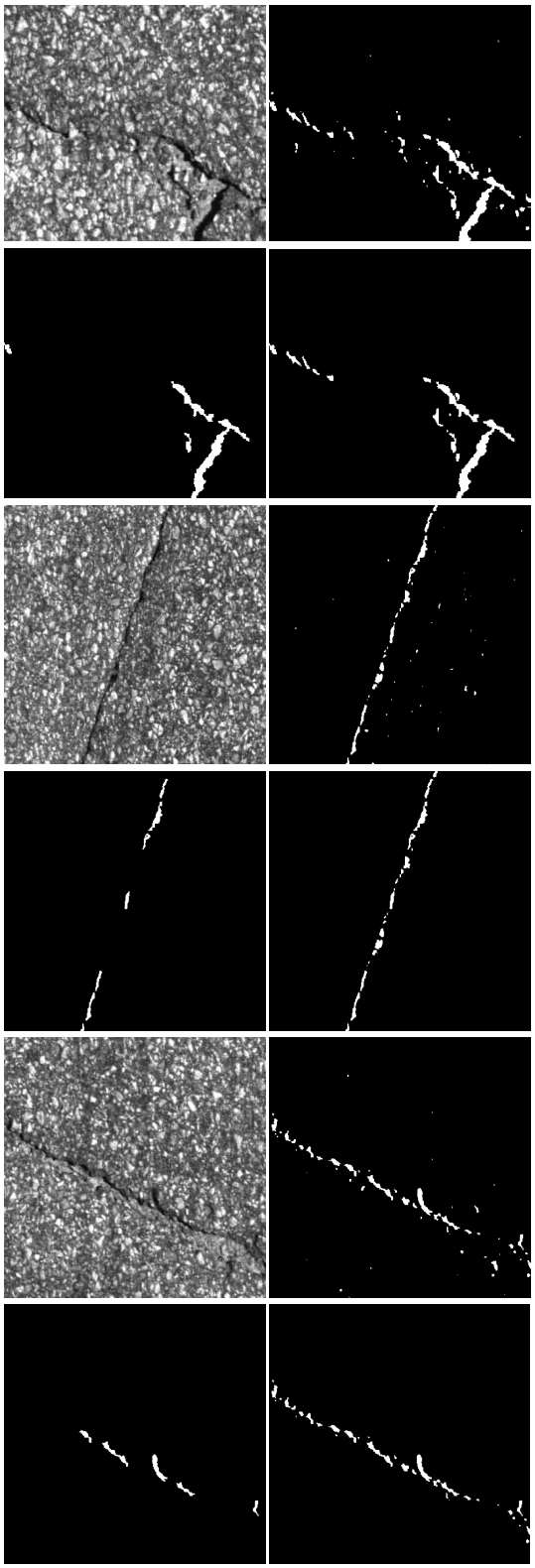

Figure 11: Connected components linkage results. Each pair of rows (from left to right and top to bottom) represents: original image; segmentation result; the connected components identified as relevant; the final crack regions detection after the proposed linkage.

5. ACKNOWLEDGMENTS

The authors acknowledge the support from Fundação para a Ciência e Tecnologia (FCT) and also from INO [4], represented by Mr. John Laurent, for allowing the usage of the imagery database, for nonprofit research work.

REFERENCES

[1] T. Nguyen, M. Avila, and B. Stephane, "Automatic Detection and Classification of Defect on Road Pavement Using Anisotropy Measure," in *17th European Signal Processing Conference - EUSIPCO*, Glasgow, Scotland, 2009.

[2] S. Chambon, P. Subirats, and J. Dumoulin, "Introduction of a Wavelet Transform Based on 2D Matched Filter in a Markov Random Field for Fine Structure Extraction: Application on Road Crack Detection," in *Proceedings of the IS&T/SPIE Electronic Imaging Science and Technology*, vol. 7251, San Jose, USA, 2009, pp. 72510A-72510A-12.

[3] C. Ma, C. Zaho, and Y. Hou, "Pavement Distress Detection Based on Nonsubsampled Contourlet Transform," in *IEEE International Conference on Computer Science and Software Engineering, CSSE 2008*, Wuhan, China, 2008, pp. 28-31.

[4] (2010, Jan.) INO. [Online]. http://www.ino.ca/en-CA/Achievements/Description/project-p/laser-road-imaging.html

[5] H. Oliveira and P. L. Correia, "Automatic Road Crack Segmentation Using Entropy and Image Dynamic Thresholding," in *17th European Signal Processing Conference - EUSIPCO*, Glasgow, Scotland, 2009.

[6] J. Weickert, *Anisotropic Diffusion in Image Processing*, http://www.mia.uni-saarland.de/weickert/book.html, Ed. Stuttgart, Germany: ECMI Series, Teubner-Verlag, 1998.

[7] P. Perona and J. Malik, "Scale-space and Edge Detection Using Anisotropic Diffusion," *IEEE Transactions on Pattern Analysis and Machine Intelligence*, vol. 2(7), p. 629–639, 1990.

[8] P. Kovesi. (2010, Feb.) http://www.csse.uwa.edu.au/~pk/Research/MatlabFns/index.html.

[9] F. Torkamani-Azar and K. Tait, "Image Recovery Using the Anisotropic Diffusion Equation," *IEEE Transactions on Image Processing*, vol. 5(11), p. 1573–1578, 1996.

[10] H. Tsuji, T. Sakatani, Y. Yashima, and N. Kobayashi, "A Nonlinear Spatio-temporal Diffusion and its Application to Prefiltering in MPEG-4 Video Coding," in *Proceedings of the International Conference on Image Processing I*, Rochester, New York, USA, 2002, p. 85–88.

[11] S. Chao and D. Tsai, "Anisotropic Diffusion with Generalized Diffusion Coefficient Function for Defect Detection in Low-contrast Surface Images," *Pattern Recognition*, vol. Elsevier, 43, p. 1917–1931, 2010.

[12] N. Otsu, "Threshold Selection Method from Gray-Level Histograms," *IEEE Transactions on Systems, Man, and Cybernetics*, vol. 1(9), pp. 62-66, 1979.

[13] A. Sanz. (2008) 6th Symposium on pavement surface characteristics: SURF 2008 . [Online]. http://carbon.videolectures.net/2008/contrib/surf08_portoroz/amirola_psdca/surf08_amirola_psdca_01.pdf

[14] S. Awate and R. Whitaker, "Unsupervised, Information-Theoretic, Adaptative Image Filtering for Image Restoration," *IEEE Transactions on Pattern Analysis and Machine Intelligence*, vol. 28, pp. 364-376, Mar. 2006.